Materials and Manufacturing Processes, 28: 1124–1132, 2013

ISSN: 1042-6914 print/1532-2475 online
DOI: 10.1080/10426914.2013.773024

Modeling and Optimization of Medium-Speed WEDM Process Parameters for Machining SKD11

Guojun Zhang[1], Zhen Zhang[1], Jianwen Guo[1], Wuyi Ming[1], Mingzhen Li[1], and Yu Huang[12]

[1]*State Key Lab of Digital Manufacturing Equipment and Technology, School of Mechanical Science and Engineering, Huazhong University of Science and Technology, Wuhan, China*
[2]*Guangdong Province Key Lab of Digital Manufacturing Equipment, Dongguan, China*

This study analyzed the workpiece surface quality (Ra) and the material removal rate (MRR) on process parameters during machining SKD11 by medium-speed wire electrical discharge machining (MS-WEDM). An experimental plan for composite design (CCD) has been conducted according to methods response surface methodology (RSM) and subsequently to seek the optimal parameters. The experimental data were utilized to model MRR and Ra under optimal parameter condition by a backpropagation neural network combined with genetic algorithm (BPNN-GA) method. Eventually, the comparisons between the results from BPNN-GA and those from the RSM demonstrate that BPNN-GA method is a more effective way for optimizing MS-WEDM process parameters.

Keywords BPNN; GA; Modeling; Optimization; RSM; WEDM.

Introduction

Wire electrical discharge machine (WEDM) is a high-precision processing equipment, mainly used in the mold, instrument, and manufacturing industries. Up to now, the WEDM can be classified as high-speed WEDM (HS-WEDM) and low-speed WEDM (LS-WEDM) based on the speed of wire moving. HS-WEDM is a new product of independent innovation in China, which has taken up more than 85% of the Chinese domestic market due to the advantages of lower cost and thicker workpieces. However, LS-WEDM have more advantages in aspects like working speed, working accuracy, surface roughness and degree of automation. Therefore, numerous was here been made to narrow the gap between HS-WEDM and LS-WEDM, thus generating a new concept called medium-speed WEDM (MS-WEDM). Improving control system, high frequency power supply and operation software on the basis of HS-WEDM, MS-WEDM can be obtained, which realizes multiplicity cutting in higher capacity to achieve high machining productivity. However, because of lots of affecting factors and the randomness of process, it tough even for a skillful engineer to achieve the optimal effect [1]. An effective solution to this problem is to ascertain the relationship between the processing performance and its main parameters, and then to optimize the machining parameters. Two main methods, namely response surface methodology (RSM) and a backpropagation neural network combining with genetic algorithm method (BPNN-GA), can be proposed to solve this.

Received December 13, 2012; Accepted January 19, 2013

Address correspondence to Yu Huang, Huazhong University of Science and Technology, Wuhan 430074, China; E-mail: yuhuang.hust@gmail.com

As for RSM, Spedding and Wang [2] proposed a mathematic model by RSM with the input parameters and the output responses. Similarly, Kung and Chiang [3] established a mathematical model by RSM to predict MRR and Ra. Hewidy and El-Taweel [4] established mathematical models by RSM to optimize main process parameters of WEDM machining Inconel 601. Recently, Tzeng [5] implemented RSM to establish mathematical models of machining SKD11 by the CNC turning, and Chauhan [6] optimized of process parameters in turning of Titanium (Grade-5) Alloy by RSM. Malapati [7] implemented RSM to develop mathematical models of the process parameters on material removal rate (MRR) to increase process accuracy in electrochemical micromachining. On the other hand, as for BPNN-GA, Tzeng and Yang [8] adopted the BPNN with integrated GA in the process optimization for WEDM aiming to develop MRR and Ra. Kim [9, 10] implemented generalized regression neural network and genetic algorithm (GA) to strengthen image of material surfaces by modelling the SEM and to optimize of wavelet-filtered data. Lin [11] implemented an integrated approach based on neural network, GA, and the Taguchi method to model the weld bead geometry of gas tungsten arc.

Some recent researches, based on response surface, artificial neural network (ANN) and GA, have been compared as follows Quintana et al. [17] developed an ANN model to predict power consumption and to determine the optimal cutting parameters of milling operations, then he used a trial and error procedure and early stopping method for the architecture of the ANN in order to solve overfitting or overtraining problems. Chih-Cherng Chen et al. [18] established a statistical model to achieve the multiobjective optimization by RSM and GA. Bhargava et al. [19] proposed a hybrid multiobjective evolutionary optimization algorithm by multidimensional RBFs-based response surface method. Simultaneously, an automatic internal switching algorithm was applied to increase the Pareto approximation and reduce the redundant computation. Judging from the above, few papers are discussing the use of MS-WEDM for machining die steel SKD11 material through establishing mathematical models by RSM and BPNN-GA. So there is an urgent demand towards developing appropriate models to strengthen the performance of machining SKD11 by MS-WEDM.

In this article, the main work highlighted that mathematical models were developed to correlate the relationships of main MS-WEDM process parameters of die steel SKD11 material on MRR and Ra, and then the optimal processing parameters were obtained. This research was based on the RSM and BPNN-GA.

Experiment design and procedures

Materials

The workpiece is a 40-mm-thick block of SKD 11 alloy tool steel, which contains high carbon and high chromium, mainly used in the manufacturing of mold and in the die industry. SKD11 is composed of C: 1.50%, Cr: 12.0%, Mo: 0.80%, V: 0.7%, Mn: 0.45%, and Si: 0.25%. The yield stress is 330 MPa, the youngs modulus is 200 GPa, the hardness is 61 HRC, the electrical resistivity is 0.65 ($\Omega \cdot m$), and the thermal conductivity is 20.0 ($W/m \cdot k$).

Equipment and specimens

Figure 1 illustrates the machining equipment of MS-WEDM, and experiments were carried out on a medium-speed WEDM with maximum processing current of 10 A, maximum feed speed of 7.5 m/min, and maximum processing speed of 170 mm^2/min (Dongguan Hustinova Precision Machinery Co., Ltd., China). Moreover, the molybdenum wire diameter was 0.12 mm, and each workpiece was processed with a thickness of 0.03 mm and a length of 20 mm.

Experiment Design and Results

Generally, the MS-WEDM process contained three phrases, namely roughing, finishing, and surface finishing. Surface finishing leads to the productivity and surface quality, which means two key points must be taken into consideration simultaneously. Then the cutting speed and surface roughness are regarded as the measures of the MS-WEDM performance. In order to improve the model capacity of predicting the process results under given inputs, a reasonable input parameter setting has to be chosen. According to experience, survey, and some preliminary investigations, the machining quality of MS-WEDM is mainly influenced by inputs in Table 1.

Table 1 illustrates the values and levels of the input parameters covering the available range according to the characteristics of MS-WEDM.

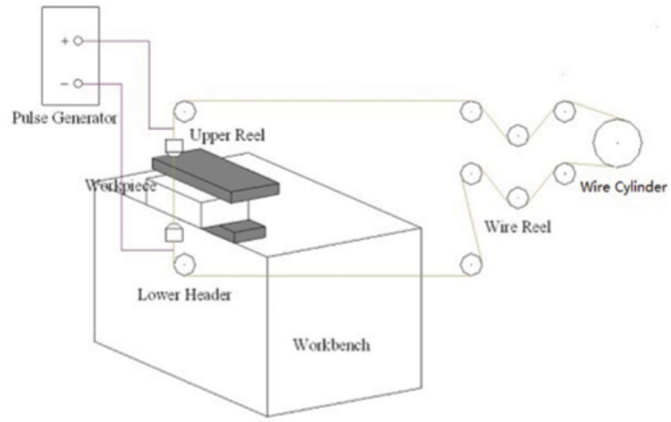

(a) Schematic drawing

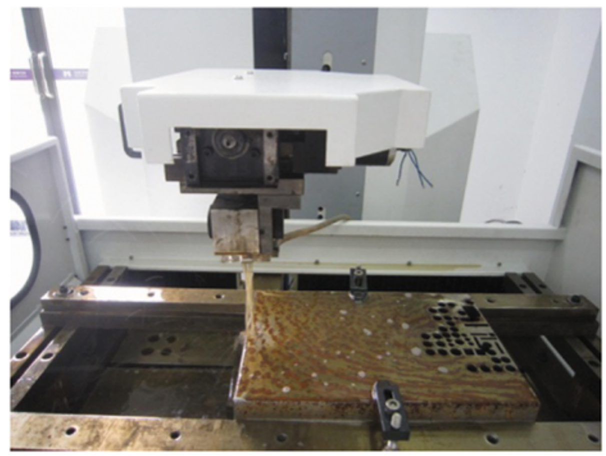

(b) Photograph of the MS-WEDM machine

Figure 1.—The experimental equipment (color figure available online).

A 5-level, 5-factor, 32-set uniform-precision central composite design (CCD) [12, 13] under coded conditions for modeling MS-WEDM process is shown in Table 2. It contains a half replication of 32 factorial design with center points and star points. RSM does not require a large number of runs or too many levels of the independent variables according to Myers and Montgomery [12]. On the other hand, especially for a practical processing experiment, the data size of 32 sets is extensive enough to develop the fitted model to find the optimum accurately. MINITAB 16 is a statistical analysis software for modelling the respond surface. Two output

Table 1.—Factors and their levels of the surface finishing.

	Level/code					
Input factors	1/-2	2/-1	3/0	4/1	5/2	unit
A-the pulse-on time :	1	3	5	7	9	µs
B-the pulse-off time :	10	25	40	55	70	µs
C-the pulse current :	1	2	3	4	5	A
D-the wire speed :	3	5	7	9	11	m/s
E-the tracking coefficient :	40	50	60	70	80	–

TABLE 2.—Results of experiment.

No.	A	B	C	D	E	v_c(mm/min)	Ra (μm)	MRR (mm^3/min)
1	3	25	2	5	70	7.69	6.1	9.228
2	7	25	2	5	50	15.38	3.627	18.456
3	3	55	2	5	50	16.67	3.28	20.004
4	7	55	2	5	70	12.5	2.66	15
5	3	25	4	5	50	20	2.92	24
6	7	25	4	5	70	25	3.489	30
7	3	55	4	5	70	16.67	2.714	20.004
8	7	55	4	5	50	34.29	3.578	41.148
9	3	25	2	9	50	14.29	2.582	17.148
10	7	25	2	9	70	30.77	2.688	36.924
11	3	55	2	9	70	30	2.562	36
12	7	55	2	9	50	46.15	2.918	55.38
13	3	25	4	9	70	42.86	2.565	51.432
14	7	25	4	9	50	42.86	3.632	51.432
15	3	55	4	9	50	46.15	2.622	55.38
16	7	55	4	9	70	46.15	4.357	55.38
17	1	40	3	7	60	44.44	3.252	53.328
18	9	40	3	7	60	46.15	3.557	55.38
19	5	10	3	7	60	50	4.187	60
20	5	70	3	7	60	42.86	3.225	51.432
21	5	40	1	7	60	34.28	2.994	41.136
22	5	40	5	7	60	52.18	2.942	62.616
23	5	40	3	3	60	34.28	3.054	41.136
24	5	40	3	11	60	38.71	2.063	46.452
25	5	40	3	7	40	34.29	1.689	41.148
26	5	40	3	7	80	30.77	1.64	36.924
27	5	40	3	7	60	27.14	1.833	32.568
28	5	40	3	7	60	30	1.801	36
29	5	40	3	7	60	30.8	1.753	36.96
30	5	40	3	7	60	31.67	1.855	38.004
31	5	40	3	7	60	30.8	1.785	36.96
32	5	40	3	7	60	31.67	1.995	38.004

Ra: Surface roughness (Ra), MRR: Material removal rate.

parameters are chosen to reflect the productivity and surface quality: MRR and surface roughness (Ra). The MRR is calculated by the following equations (Eq. 1 and Eq. 2). Then, Ra has been measured in perpendicular to the cutting direction at 0.8 mm nicks by Taylor-Hobson (Talysurf 5–120) surface roughness tester. The mean of five measured values at five different places was regarded as the result value:

$$v_c = \frac{60 \times l}{t}, \tag{1}$$

$$MRR = v_c \times H \times k, \tag{2}$$

where the v_c is the average feed rate in mm/min, a the l and the t are the cutting length in mm and time in s, respectively. The H and the k are the workpiece thickness and cutting thickness in mm, respectively, and the MRR is thus measured in mm^3/min.

OPTIMIZATION METHODOLOGIES

RSM and BPNN-GA were regarded as optimization methodologies to optimize the input parameters. Figure 2 is a flow chart showing the steps to determine an optimal process setting.

The steps in detail are as follows:

1. Identify main goals. The main goal is to obtain an optimal setting to minimize Ra and maximize MRR.
2. Design experiments. A 5-level, 5-factor, 32-set CCD was used to carry out the experiment.
3. Experiment and measurement. The experimental plan was conducted on MS-WEDM corresponding to CCD table, while MRR and Ra were obtained.
4. Optimization process parameters. The process model was developed to achieve an optimal parameter by RSM and BPNN-GA methods.
5. Result comparison. Compared the optimal parameters of the RSM with that of the BPNN-GA, confirmation experiment was carried out.

RSM Technique

RSM can be proposed to solve the correlation of input parameters with outputs of MS-WEDM processing.

The general second-order polynomial response is described in Eq. 3:

$$Y = \beta_0 + \sum_{i=1}^{p} \beta_i x_i + \sum_{i=1,j=1}^{p} \sum_{i<j}^{p} \beta_{ij} x_i x_j + \sum_{i=1}^{p} \beta_{ii} x_i^2 + \epsilon, \tag{3}$$

where Y is the measured response, β_0 is the constant term which is estimated by mean of minimum squares, β_i is the linear effect, β_{ij} is the interactive effect of x_j

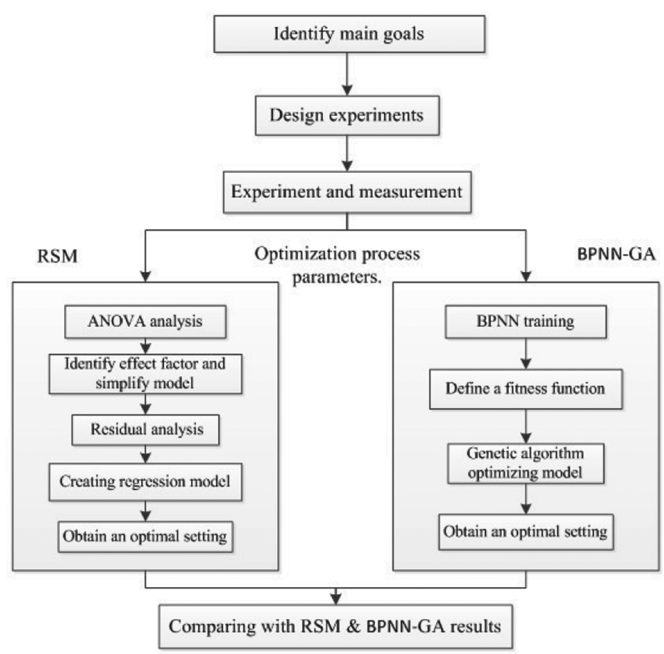

FIGURE 2.—Flow chart of obtaining optimal process.

and x_i (input variables), β_{ii} is the second order effect, and ϵ is the experimental random error component.

In the present study, a second-order predictive model about input parameters and the responses of MS-WEDM was established by the RSM due to the high predictability of this model. Then the adequacy of this second-order predictive model was verified by the analysis of variance (ANOVA). Montgomery [12] described that $P < 5\%$ (at 95% confidence level) manifests that the optimal model is believed to be appropriate and significant in statistics.

Mathematical predictive model developed for Ra. The ANOVA for the complete second-order fitted model of Ra (Table 3 as follows) illustrated the term of E*E (P = 0.6) is insignificant effect and should be removed from predictive model in order to avoid the underfitting or lack of fit problem. After removing the term of E*E, the simplified model was better and more accurate according to Table 3. Most of the values of P are less than 0.05, which means that the model is effective.

Analyzing residuals with residual plot (Fig. 3(a)) is a valid method to prove whether the developed model is accurate or not. Residual plot has four parts which are normal probability plot (Fig. 3(a)a), scatter diagram of fitted values (Fig. 3(a)b), histogram of residuals (Fig. 3(a)c) and scatter diagram of observation sequence (Fig. 3(a)d). Normal probability plot (Fig. 3a) and histogram of residuals (Fig. 3(a)c) demonstrate that residuals fit normal distribution. Scatter diagram of fitted values (Fig. 3(a)b) shows that residuals keep homogeneity of variance and shape infundibula. Scatter diagram of observation sequence (Fig. 3(a)d) illustrates that scatter dots fluctuate randomly and irregularly between top and bottom of a horizontal axis without abnormal trend. It can be confirmed that developed model is reasonable normal through analyzing residual plot.

The analysis above demonstrates that the second-order model for Ra is appropriate to express the MS-WEDM process. The equation to obtain Ra is as follows (Eq. 4).

$$
\begin{aligned}
Ra = {} & 21.9112 - 1.86286A - 0.291579B - 4.39521C \\
& - 1.95097D + 0.140665E + 0.105211A^2 + 0.00220542B^2 \\
& + 0.311719C^2 + 0.0063875A \times B + 0.214563A \times C \\
& + 0.0769375A \times D - 0.00968125A \times E + 0.017675B \\
& \times C + 0.0102B \times D - 0.0000911B \times E + 0.1685C \\
& \times D - 0.0076875C \times E - 0.0035625D \times E \qquad (4)
\end{aligned}
$$

Then optimal parameters setting and optimization diagram on Ra obtained by the RSM are as follows (Table 4).

TABLE 3.—ANOVA for Ra (μm) of the complete and simplified second-order model.

	The complete model						The simplified model					
Source	DOF	Seq SS	Adj SS	Adj MS	F	P	DOF	Seq SS	Adj SS	Adj MS	F	P
Regression	20	27.552	27.5552	1.37776	57.37	0	19	27.5483	27.5483	1.44991	64.16	0
Liner	5	3.0624	3.0624	0.61248	25.5	0	5	3.0624	3.0624	0.61248	27.1	0
A	1	0.2042	0.2042	0.20424	8.5	0.014	1	0.2042	0.2042	0.20424	9.04	0.011
B	1	0.9745	0.9745	0.97445	40.58	0	1	0.9745	0.9745	0.97445	43.12	0
C	1	0.0173	0.0173	0.01728	0.72	0.414	1	0.0173	0.0173	0.01728	0.76	0.399
D	1	1.7195	1.7195	1.71949	71.6	0	1	1.7195	1.7195	1.71949	76.09	0
E	1	0.147	0.147	0.14695	6.12	0.031	1	0.147	0.147	0.14695	6.5	0.025
Square	5	13.9293	13.9293	2.78587	116	0	4	13.9223	13.9223	3.48059	154.03	0
A*A	1	3.7388	5.1635	5.16349	215	0	1	3.7388	5.2315	5.23154	231.51	0
B*B	1	6.2923	7.1854	7.18542	299.2	0	1	6.2923	7.2733	7.27335	321.87	0
C*C	1	2.5967	2.8268	2.82679	117.71	0	1	2.5967	2.8702	2.87021	127.02	0
D*D	1	1.2945	1.2698	1.26977	52.87	0	1	1.2945	1.2945	1.29452	57.29	0
E*E	1	0.007	0.007	0.007	0.29	0.6	–	–	–	–	–	–
Interaction	10	10.5635	10.5635	1.05635	43.99	0	10	10.5635	10.5635	1.05635	46.75	0
A*B	1	0.5875	0.5875	0.58752	24.46	0	1	0.5875	0.5875	0.58752	26	0
A*C	1	2.9464	2.9464	2.94637	122.69	0	1	2.9464	2.9464	2.94637	130.39	0
A*D	1	1.5154	1.5154	1.51536	63.1	0	1	1.5154	1.5154	1.51536	67.06	0
A*E	1	0.5999	0.5999	0.59985	24.98	0	1	0.5999	0.5999	0.59985	26.55	0
B*C	1	1.1247	1.1247	1.12466	46.83	0	1	1.1247	1.1247	1.12466	49.77	0
B*D	1	1.4982	1.4982	1.49818	62.38	0	1	1.4982	1.4982	1.49818	66.3	0
B*E	1	0.2987	0.2987	0.29866	12.44	0.005	1	0.2987	0.2987	0.29866	13.22	0.003
C*D	1	1.8171	1.8171	1.8171	75.66	0	1	1.8171	1.8171	1.8171	80.41	0
C*E	1	0.0946	0.0946	0.09456	3.94	0.073	1	0.0946	0.0946	0.09456	4.18	0.063
D*E	1	0.0812	0.0812	0.08122	3.38	0.093	1	0.0812	0.0812	0.08122	3.59	0.082
Residual error	12	0.2642	0.2642	0.02402			12	0.2712	0.2712	0.0226		
Total	31	27.8194					31	27.8194				

DOF: Degrees of freedom, Seq SS: sequential sum of squares, Adj SS: adjusted sum of squares, Adj MS: adjusted mean squares.

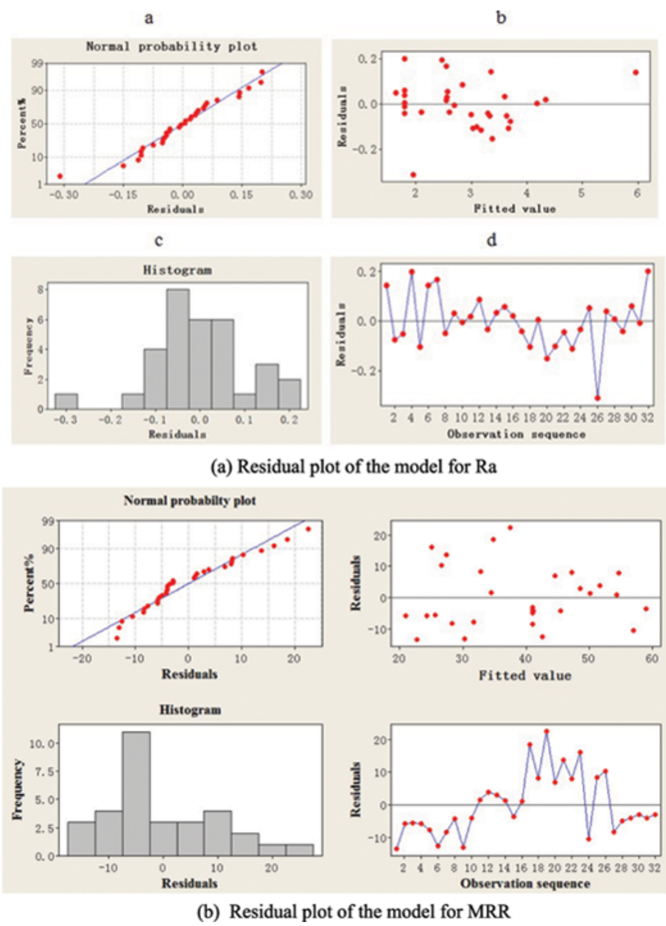

FIGURE 3.—Residual plot for Ra (μm) and MRR (mm^3/min) (color figure available online).

Mathematical predictive model developed for MRR. With the same method as the above, Table 5 of the ANOVA for the MRR with simplified second-order model can be achieved. The P values of some terms are more than 0.05 in the Table 5, which means this simplified second Corder model by RSM is not very significant. On the other hand, after analyzing residuals with residual plot (Fig. 3(b)), it can be concluded that residuals fit normal distribution and keep homogeneity of variance. So this model still has certain value for reference to optimal parameters setting.

The analysis above demonstrates that the second-order model for MRR is also appropriate for expressing the MS-WEDM process. The equation to obtain MRR

TABLE 4.—Optimal setting on Ra (μm) and MRR (mm^3/min).

Method	Input factor	Pulse-on time	Pulse-off time	Pulse current	Wire speed	Tracking coefficient	Predicted value
RSM	Ra	3.1	34.85	2.66	10.4	40	1.1
	MRR	9	70	5	11	43.6	95.8
BPNN-GA	Ra	5.02	42.66	2.14	10.9	45.45	1.69
	MRR	7.31	33.94	1.82	10.44	47.04	69.25

TABLE 5.—ANOVA for MRR (mm^3/min) after simplifying the model.

Source	DOF	Seq SS	Adj SS	Adj MS	F	P
Regression	8	3552.85	3552.85	444.11	3.74	0.006
Liner	5	3014.87	3014.87	602.97	5.08	0.003
A	1	232.06	232.06	232.06	1.96	0.175
B	1	75.4	75.4	75.4	0.64	0.434
C	1	1115.15	1115.15	1115.15	9.4	0.005
D	1	1533.89	1533.89	1533.89	12.92	0.002
E	1	58.37	58.37	58.37	0.49	0.49
Square	1	238.12	238.12	238.12	2.01	0.17
E*E	1	238.12	238.12	238.12	2.01	0.17
Interaction	2	299.87	299.87	149.93	1.26	0.302
B*D	1	59.03	59.03	59.03	0.5	0.488
B*E	1	240.84	240.84	240.84	2.03	0.168
Residual error	23	2729.57	2729.57	118.68		
Total	31	6282.42				

is as follows (Eq. 4):

$$\begin{aligned} MRR = {} & -156.127 + 1.55475A + 1.22189B + 6.81650C \\ & + 1.43625D + 4.25941E - 0.028173E^2 \\ & + 0.064025B \times D - 0.025865B \times E. \end{aligned} \tag{5}$$

Then optimal parameters setting and optimization diagram on MRR obtained by the RSM as follows (Table 4).

Optimization Method of with BPNN-GA

BPNN has the capacity to solve incomplex nonlinear problems such as modeling, prediction, optimization, and adaptive control [14]. While GA has the capacity of multiparameter optimization in many research fields.

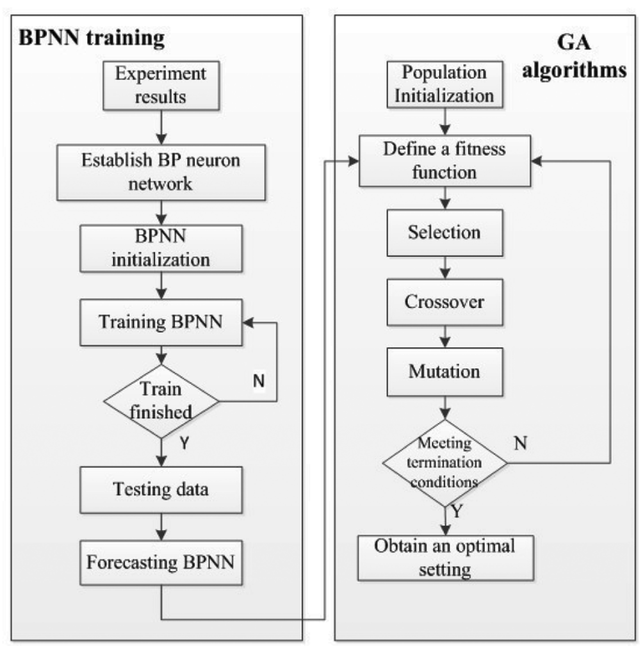

FIGURE 4.—Flow chart of the BPNN-GA.

TABLE 6.—The effects of different numbers of hidden neurons on the BPNN for Ra (μm) and MRR (mm^3/min).

Network	No.of 1st	No.of 2nd	Mean error of Ra (%)	Mean error of MRR (%)
SHL network	7	–	35.13(%)	21.02(%)
	8	–	18.00(%)	21(%)
	9	–	25.11(%)	25.01(%)
DHL network		5	–	12.31(%)
	7	6	–	24.28(%)
		7	–	22.13(%)
		3	23.12(%)	19.69(%)
	8	4	14.57(%)	17.50(%)
		5	22.14(%)	16.16(%)
		5	23.31(%)	–
	9	6	27.60(%)	–
		7	27.45(%)	–

SHL network: single-hidden-layer network, DHL network: double-hidden-layer network, No.of 1st: No.of neurons in 1st hidden layer, No.of 2nd: No.of neurons in 2nd hidden layer.

Zemin [15] considered that BPNN-GA has been applied to develop the traditional ANN for multiparameter optimization problems. In a word, BPNN-GA is an optimization approach that combines the capacity of nonlinear fitting of neural network with the capacity of nonlinear optimizing of genetic algorithm. In the BPNN-GA, predicted results of BPNN after training is regarded as the fitness value of individual, and then optimal results can be achieved after the operation of reproduction, crossover and mutation.

Fig. 4 is a flow chart showing how to obtain an optimal process by the BPNN-GA. The platform to create the BP and was based on MATLAB Neural Network Toolbox.

The complete BPNN is made up of an input layer, hidden layers, and an output layer. The experimental results with expansions were regarded as inputs of the neural networks for training. Input vectors contained A, B, C, D, and E, output vectors consisted of Ra or MRR. The hyperbolic tangent and linear transfer function were

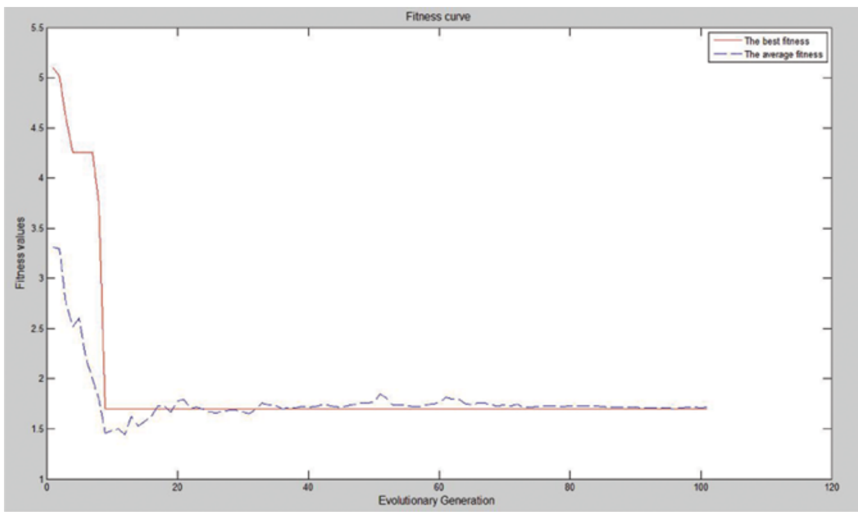

(a) Fitness curve of Ra(μm) by BPNN-GA

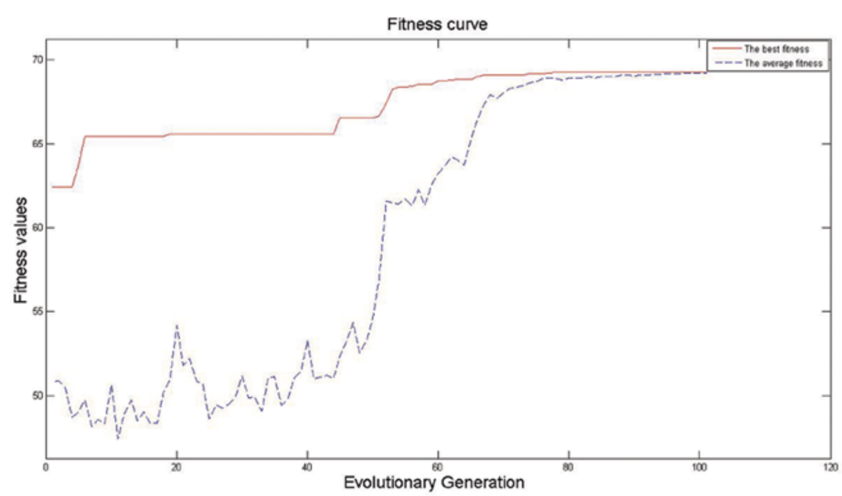

(b) Fitness curve of MRR by BPNN-GA

FIGURE 5.—Fitness curve of Ra (μm) and MRR (mm^3/min) (color figure available online).

separately utilized for the hidden and output layers. Additionally, the convergence function (Eq. 6) (used for judging train finish) is

$$MSE = \frac{1}{N}\sum_{i=1}^{N}(d_i - y_i)^2, \tag{6}$$

Where MSE is the mean squared error, N is the number of experimental points, and d_i and y_i are, respectively, the values of experimental and predicted value in training sample i.

The number of the hidden layers of BPNN should be taken into consideration [16]. To achieve the best value of Ra or MRR under optimal input setting, single and double hidden-layer networks with different neurons were trained, respectively, and then their results were examined and compared to find the most suitable model. It is concluded from Table 6 that the mean error of 14.57% for Ra is available in the best case of 5-8-4-1 neural networks. Simultaneously, it is also concluded from table 6 that the mean error of 12.31% for MRR is available in the best case of 5-7-5-1 neural networks.

On the other hand, GA is used as a nonlinear optimizing method to find out the best extremum. GA adopted real coding as individuals and the length of individual was 5 corresponding to 5 input parameters. Fitness values of individuals were predictive values of BPNN. The roulette wheel method was selected for reproduction. Simultaneously, the crossover probability was 0.4 by two-point approach, and the mutation rate was 0.2. Fig. 5a and Fig. 5b show the fitness curve of Ra and MRR by BPNN-GA including the best fitness and average fitness. An optimal combination of process parameters is achieved via the BPNN-GA as in (Table 4).

Result and discussion

Influence of Cutting Conditions on Ra and MRR

Through observing and analyzing all the surface plots of RSM, the best surface plot (Fig. 6) was selected according to the significance of input factors for Ra. It apparent that A and B have a significant impact on response variable Ra for the reason that change trend of surface plot (Fig. 6a) is extremely steep. There exists the bottom dot in the response surface plot which means the smallest Ra with the combination of input factors (A and B). In the 3D surface plot (Fig. 6b), it is concluded that when the values of A and B choose medium numbers (B is about 40 and A is between 2.5 and 5), Ra is smaller than the situation when A and B are boundary values. The higher discharge energy destroys too much and explodes with spark and gas bubbles on the finished surface at the long time of pulse-on, while the lower energy is insufficient to destroy the workpiece surface at the long time of pulse-off. Simultaneously, through observing and analyzing all the surface plots for MRR, the best surface plot (Fig. 7) was chosen. It is apparent that D (wire speed) and E (tracking coefficient) have a significant effect on MRR for the same reason. There also exists

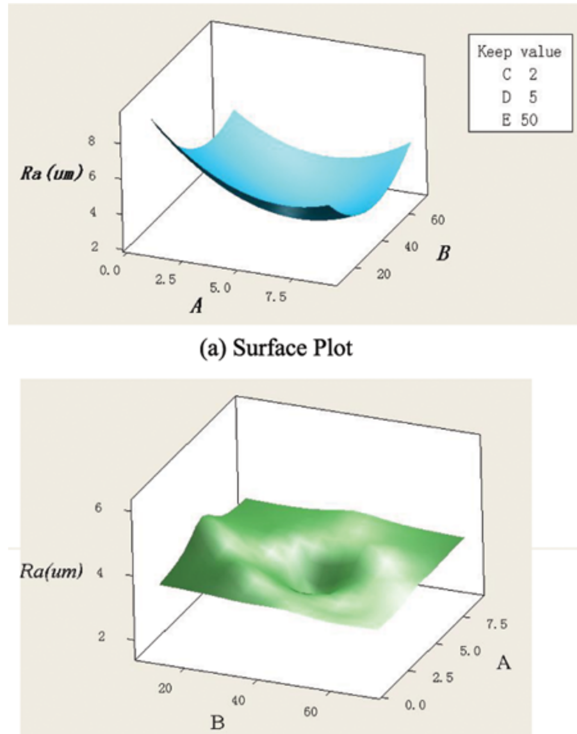

(a) Surface Plot

(b) 3D Surface Plots

Figure 6.—Surface plot of Ra (μm) with A and B (color figure available online).

the top dot in the response surface plot which means the largest MRR with the combination of control factors (D and E). In the 3D surface plot (Fig. 7b), it is concluded that when the values of D increase and E is the medium number, MRR becomes larger. Increasing wire speed can result in decreasing in the rate of wire abrasion so as to enhance the efficiency of machining hard surface. Tracking coefficient, which controls the feed speed and adjusts the gap between workpiece and wire, has a significant impact on MRR.

Comparison of the Two Methods and Confirmation

Two different approaches were utilized to optimize process parameters and obtain optimal combination of process parameters for Ra and MRR, respectively. Confirmation experiment should be conducted to compare and judge which optimization approach is more effective and significant, and then to verify the conclusions which are described from the analysis phase. The results of confirmation experiments under the optimal combination of process parameters are listed in Tables 7 and 8. The relative residuals of Ra and MRR from RSM are 33.3% and 53.28%, respectively, while the relative residuals of Ra and MRR from BPNN-GA are 1.2% and 5.24%, respectively. By comparison of residuals from RSM and BPNN-GA, as for the optimal models on Ra and MRR, the applied BPNN-GA approach gives more accurate results of prediction and confirmation than the RSM approach.

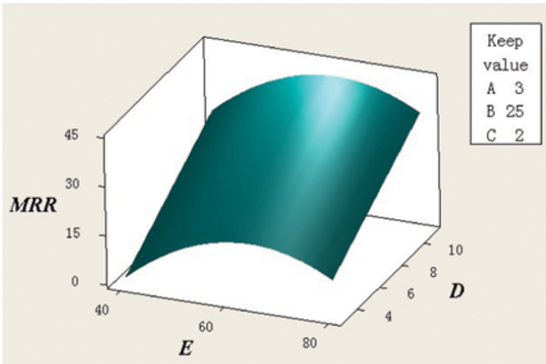

(a) Surface Plot

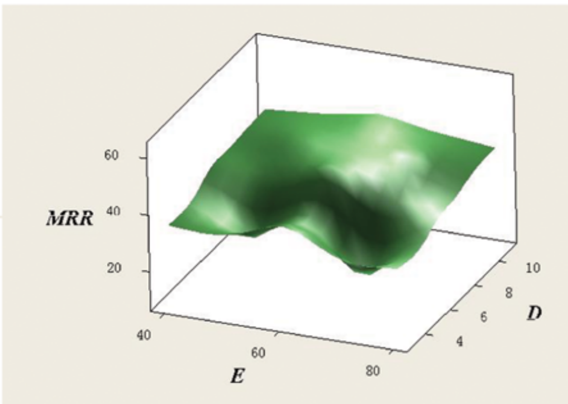

(b) 3D Surface Plots

FIGURE 7.—Surface plot of MRR (mm^3/min) with D and E (color figure available online).

In this study, the most appropriate architecture of neural network was developed by method of trial and error. Evolutionary neural network (EVONN) [20, 21] has become a popular multiobjective optimization approach to configure the most suitable weights and topology by using predatorc-prey GA and a Pareto frontier. The most suitable network

TABLE 7.—Results of confirmation experiment on Ra (μm).

	Optimal parameters					Ra		
Applied method	A	B	C	D	E	Predicted	Exp.	Relative residual
RSM	3.1	34.85	2.66	10.4	40	1.1	1.65	33.3%
BPNN-GA	5.02	42.66	2.14	10.9	45.45	1.69	1.71	1.2%

TABLE 8.—Results of the experimental confirmation on MRR (mm^3/min).

	Optimal parameters					MRR		
Applied method	A	B	C	D	E	Predicted	Exp.	Relative residual
RSM	9	70	5	11	43.6	95.8	62.5	53.28%
BPNN-GA	7.31	33.94	1.82	10.44	47.04	69.25	65.8	5.24%

is achieved through Akaike information criterion (AIC), Bayesian information criteria (BIC), or the final prediction error (FPE) to avoid overfitting and underfitting problems. This approach had been applied successfully in some different manufacturing fields and would be a good alternative to BNPP-GA model of this. On the other hand, as for multiobjective optimization, EVONN has been extended to genetic programming (GP), which is emerging as an efficient alternate of ANN [22, 23]. To develop a data-driven model, GP [22] can construct the mathematical function (encoded as tree) between inputs and responses by the use of a function set and a terminal set. However, the conventional GP has some defects: the lower error tree may lead to overfitting problems, while the larger error could result in underfitting problems. Therefore, a new GP technique, the bi-objective evolutionary genetic programming (BioGP), was proposed. A complex and accurate metamodel can be constructed by the BioGP approach [23] which can not only minimize training error based on a single objective optimization strategy but also work out an appropriate trade-off between training error and complexity of the GP trees. The experimental work of this article is extensive enough to offer the accurate and practical methods, so the use of EVONN, GP, or BioGP is less necessary. But these methods have provided some good options to deal with the data-driven modeling and the multiobjective optimization.

CONCLUSION AND FUTURE WORK

The present research proposed an effective approach and framework of optimizing process parameters of machining SKD11 that integrates RSM with BPNN-GA. The proposed approach and framework can give the optimal process parameter settings on Ra and MRR for MS-WEDM machining SKD11, respectively. The following conclusions are drawn from the present researcher:

1. RSM indicates that pulse-on and pulse-off time are two most significant factors for Ra, while wire speed and tracking coefficient are two most significant factors for MRR. The higher values of pulse-on time or wire speed generate rougher surfaces (decreases Ra) and increases MRR.
2. The integrated BPNN-GA approach applied is utilized to achieve the optimal parameter settings of Ra and MRR for MS-WEDM process. In addition, as for the optimal models on Ra and MRR, the BPNN-GA approach shows more accurate results of prediction and confirmation than the RSM approach.
3. The predicted accuracy of BPNN has a closed relationship with the significance of optimal results. In other words, due to predicted results of the trained BPNN being regarded as the fitness value of individual, the optimal results can be achieved by the nonlinear optimizing of GA. The more accurately BPNN predicted, the more effective and significant optimal results are.

4. In this article, Ra and MRR are respectively regarded as output response in the optimal model. In the future work, the relationship of cutting conditions and surface crack formation, such as whiter layer, crack, and microsurface topography, will be investigated. In addition, one computer-aided process planning (CAPP) system, which guides process in order to optimize cutting conditions, will be built in the MS-WEDM.

Acknowledgement

This research was supported by the National Natural Science Foundation of China (NSFC) under Grant No. 51175207 and Grant No. 51121002, the National Key Technology R&D Program No. 2012BAF13B07, and the Science and Technology Planning Project of Guangdong Province No. 2012B011300015. Authors Guojun Zhang and Zhen Zhang contributed equally to this work.

References

1. Williams, R.E.; Rajurkar, K.P. Study of wire electrical discharge machining surface characteristics. *Journal of Materials Processing Technology* **1991**, *28*, 127–138.
2. Spedding, T.A.; Wang, Z.Q. Study on modeling of wire EDM process. *Journal of Materials Processing Technology* **1997**, *69*, 18–28.
3. Kung, K.Y.; Chiang, K.T. Modeling and analysis of machinability evaluation in the wire electrical discharge machining (WEDM) process of aluminum oxide-based ceramic. *Materials and Manufacturing Processes* **2008**, *23*, 241–250.
4. Hewidy, M.S.; El-Taweel, T.A.; El-Safty, M.F. Modelling the machining parameters of wire electrical discharge machining of Inconel 601 using RSM. *Journal of Materials Processing Technology* **2005**, *169*, 328–C336.
5. Tzeng, C.J.; Yang, Y.K. Determination of optimal parameters for SKD11 CNC turning process. *Materials and Manufacturing Processes* **2008**, *23* (4), 363–368.
6. Chauhan, S.R.; Dass, K. Optimization of machining parameters in turning of titanium (grade-5) alloy using response surface methodology. *Materials and Manufacturing Processes* **2012**, *27* (5), 531–537.
7. Malapati, M.; Bhattacharyya, B. Investigation into electrochemical micromachining process during micro-channel generation. *Materials and Manufacturing Processes* **2011**, *26* (8), 1019–1027.
8. Tzeng, C.J.; Yang, Y.K. Optimization of wire electrical discharge machining of pure tungsten using neural network and response surface methodology. *Proceedings of the Institution of Mechanical Engineers Part B: Journal of Engineering* **2011**, DOI: 10.1243/09544054JEM2021.
9. Kim, B.; Kim, D. Use of neural network and genetic algorithm to model scanning electron microscopy for enhanced image of material surfaces. *Materials and Manufacturing Processes* **2011**, *26* (3), 382–387.
10. Kim, B.; Kim, D. Optimization of Wavelet-filtered In-situ plasma etch data using neural network and genetic algorithm. *Materials and Manufacturing Processes* **2011**, *26* (3), 398–402.
11. Lin, H.L.; Chou, C.P. Optimization of the GTA welding process using combination of the taguchi method and a Neural-genetic approach. *Materials and Manufacturing Processes* **2010**, *25* (7), 631–636.
12. Montgomery, D.C. *Design and Analysis of Experiments*; Wiley: Hoboken, 2001.
13. Rahman, M.M.; Khan, M.A.R. Optimization of machining parameters on surface roughness in EDM of Ti-6Al-4 V using response surface method. *Advanced Materials Research* **2011**, *213*, 402–408.
14. Freeman, J.A.; Skapura, D.M. *Neural networks: Algorithms, applications, and programming techniques*; Addison Wesley: Reading, Massachusetts, 1992.
15. Zemin, F.; Jianhua, M. Back prediction of high-strength sheet metal under air bending forming and tool design based on GACBPNN. *International Journal of Advanced Manufacturing Technology* **2011**, *53* (5C8), 473–C483.
16. Assarzadeh, S.; Ghoreishi, M. Neural-network-based modeling and optimization of the electro-discharge machining process. *International Journal of Advanced Manufacturing Technology* **2008**, *39*, 488–C500.
17. Quintana, G.; Ciurana, J.; Ribatallada, J. Modelling power consumption in Ball-end milling operations. *Materials and Manufacturing Processes* **2011**, *26* (5), 746–756.
18. Chen, C.-C.; Su, P.-L.; et al. Experimental investigation of designed parameters on dimension shrinkage of injection molded Thin-wall part by integrated response surface methodology and genetic algorithm: A case study. *Materials and Manufacturing Processes* **2011**, *26* (3), 534–540.
19. Bhargava, S.; Dulikravich, G.S.; Murty, G.S.; et al Stress corrosion cracking resistant aluminum alloys: Optimizing concentrations of alloying elements and tempering. *Materials and Manufacturing Processes* **2011**, *26* (3), 363–374.
20. Pettersson, F.; Chakraborti, N.; Saxen, H. A genetic algorithms based multi-objective neural net applied to noisy blast furnace data. *Applied Soft Computing* **2007**, *7* (1), 387–397.
21. Mondal, D.N.; Sarangi, K.; Pettersson, F.; et al. Cu-Zn separation by supported liquid membrane analyzed through Multi-objective genetic algorithms. *Hydrometallurgy 107* (3–4), 112–123.
22. Biswas, A.; Maitre, O.; Mondal, D.N.; Das, S.K.; Sen, P.K.; Collet, P.; Chakraborti, N. Data-driven multiobjective analysis of manganese leaching from low grade sources using genetic algorithms, genetic programming, and other allied strategies. *Materials and Manufacturing Processes* **2011**, *26* (3), 415–430.
23. Brijesh, K.G.; Jussi, H.; Kaisa, M.; Nirupam, C. Genetic programming through bi-objective genetic algorithms with a study of asimulated moving bed process involving multiple objectives. *Applied Soft Computing* **2013**, *13* (5), 2613–2623.